applied sciences

MDPI

Article

Approximation of the Mechanical Response of Large Lattice Domains Using Homogenization and Design of Experiments

Diego Montoya-Zapata [1,2], Diego A. Acosta [3], Camilo Cortés [2,*], Juan Pareja-Corcho [1,2], Aitor Moreno [2], Jorge Posada [2] and Oscar Ruiz-Salguero [1]

1 Laboratory of CAD CAM CAE, Universidad EAFIT, Cra 49 no 7-sur-50, Medellín 050022, Colombia; dmonto39@eafit.edu.co (D.M.-Z.); jpareja1@eafit.edu.co (J.P.-C.); oruiz@eafit.edu.co (O.R.-S.)
2 Vicomtech Foundation, Basque Research and Technology Alliance (BRTA), Mikeletegi 57, 20009 Donostia-San Sebastian, Spain; amoreno@vicomtech.org (A.M.); jposada@vicomtech.org (J.P.)
3 Grupo de Diseño y Desarrollo de Procesos (DDP), Universidad EAFIT, Cra 49 no 7-sur-50, Medellín 050022, Colombia; dacostam@eafit.edu.co
* Correspondence: ccortes@vicomtech.org; Tel.: +34-943-309-230

Received: 26 March 2020; Accepted: 26 May 2020; Published: 1 June 2020

Abstract: Lattice-based workpieces contain patterned repetition of individuals of a basic topology (Schwarz, ortho-walls, gyroid, etc.) with each individual having distinct geometric grading. In the context of the design, analysis and manufacturing of lattice workpieces, the problem of rapidly assessing the mechanical behavior of large domains is relevant for pre-evaluation of designs. In this realm, two approaches can be identified: (1) numerical simulations which usually bring accuracy but limit the size of the domains that can be studied due to intractable data sizes, and (2) material homogenization strategies that sacrifice precision to favor efficiency and allow for simulations of large domains. Material homogenization synthesizes diluted material properties in a lattice, according to the volume occupancy factor of such a lattice. Preliminary publications show that material homogenization is reasonable in predicting displacements, but is not in predicting stresses (highly sensitive to local geometry). As a response to such shortcomings, this paper presents a methodology that systematically uses design of experiments (DOE) to produce simple mathematical expressions (meta-models) that relate the stress–strain behavior of the lattice domain and the displacements of the homogeneous domain. The implementation in this paper estimates the von Mises stress in large Schwarz primitive lattice domains under compressive loads. The results of our experiments show that (1) material homogenization can efficiently and accurately approximate the displacements field, even in complex lattice domains, and (2) material homogenization and DOE can produce rough estimations of the von Mises stress in large domains (more than 100 cells). The errors in the von Mises stress estimations reach 42% for domains of up to 24 cells. This result means that *coarse* stress–strain estimations may be possible in lattice domains by combining DOE and homogenized material properties. This option is not suitable for *precise* stress prediction in sensitive contexts wherein high accuracy is needed. Future work is required to refine the meta-models to improve the accuracies of the estimations.

Keywords: design of experiments; lattice structures; homogenization; schwarz primitive; mechanical characterization; modeling and simulation

1. Introduction

New emerging technologies in the context of Industry 4.0, such as digital twins, pose new challenges in the design and simulation in the industrial and biomedical ecosystems. The interactive nature of the processes of Industry 4.0 requires fast simulation methods that enable real-time decision making and digital twins being continuously updated with the physical world [1].

Lattice materials have multiple applications in engineering (e.g., energy absorption) and biomedicine (e.g., implants and scaffolds) [2]. However, the simulation of large lattice domains is in many cases unfeasible because: (1) the meshing of these domains is a time consuming process that involves human intervention and (2) the size of the produced meshes is intractable due to the geometric complexity associated with these domains [3,4].

This manuscript implements a methodology that combines material homogenization and design of experiments (DOE) to estimate the stress–strain response in large lattice domains. The main advantage of this methodology is its lesser computational demands in comparison to finite element analysis (FEA). We apply this approach to approximate the von Mises stress in lattice structures of the type Schwarz primitive. This manuscript is an extension of the work in [5] which presents a methodology to develop the meta-models using DOE but does not integrate them with material homogenization to produce stress–strain estimations in large lattice domains.

The remainder of this article is organized as follows: Section 2 provides a review of the relevant related work. Section 3 describes the proposed methodology to estimate the stress–strain response in lattice domains using material homogenization and DOE. Section 4 presents and evaluates the results of the implementation of our methodology. Section 5 concludes the manuscript and suggests future extensions of the article.

2. Literature Review

2.1. Lattice Structures and Material Homogenization

Lattice structures are generally composed of replicas of a unit cell that are continuous, uniformly distributed and fill the space. The reason why lattice structures attract the attention of engineers is that they can retain good mechanical performance while reducing material usage and weight. For this reason, lattice structures are used for energy absorption, heat transfer and vibration damping applications [2]. Additive manufacturing (AM) has also widened the application range of lattice structures. The manufacturing freedom of AM has promoted the use of lattice structures for materializing the results of structural optimization [6–9] and for biomedical applications in orthopedics and tissue engineering [10,11].

Material homogenization seeks the equivalent Young's modulus and Poisson's ratio to produce a homogeneous structure that resembles the displacements field of the lattice domain. Material homogenization suppresses the geometrical complexity associated with lattice domains. Therefore, lighter FEA meshes are obtained, and consequently, the computational cost and time requirements for FEA simulations are reduced [6,12].

Apart from predicting macro-mechanical properties (Young's and Poisson's moduli), material homogenization has enabled the study of periodic strut-like lattice structures built via AM, considering the defects caused during the manufacturing with AM and the stiffening in the joints of the structure [13,14]. These studies are, however, limited to strut-like lattice structures. Material homogenization has also been successfully integrated with topology optimization to produce optimal designs of lattice structures suitable for AM [6,12]. However, since the homogeneous and lattice domains have notorious geometrical differences and stresses/strains depend on the geometry, the stress–strain behavior of the homogeneous domain does not resemble the one of the lattice domain.

2.2. Modeling and Simulation of Lattice Structures

The numerical analysis of the mechanical behavior of large lattice structures is challenging due to the high computing (memory and time) requirements [4]. Large lattice structures demand heavy FEA meshes formed by solid elements. Sometimes solid FEA meshes can be simplified using simpler and lighter FEA elements (beams or shells). This approach has allowed for simulations of relatively large domains of a few hundred of cells [4,15–17]. However, this technique cannot be applied to surface-type lattice structures like Schwarz primitive lattices, since this kind of architecture cannot be approximated by long struts or thin plates.

Regarding the joint use of FEA and DOE, we found that they have been combined in several applications in non-lattice structures. The current work can be divided into three groups: (i) evaluation of material and mechanical properties, including metals [18], resins [19] and composite materials [20]; (ii) shape optimization of mechanical parts, including medical devices [21] and automobile parts [22]; and (iii) generation of meta-models to estimate the stress–strain responses in small lattice domains using DOE [5]. However, the produced meta-models are not used for any further analysis with large lattice domains. To the best of our knowledge, the works in the literature do not implement a methodology that integrates systematically material homogenization and DOE for stress–strain estimation in the field of lattice materials.

Monte Carlo methods [23,24] use random samples in the domains of input variables for an experiment. The experiment is run under the prescribed combination of input variables, and the resulting output values recorded. The model mathematical model for the system or cause/effect is computed on the basis of maximal likeness. In our case, the expenses of running each test are significant since each test requires the preparation and setup of the FEA experiment; the execution itself and its post-processing; and the analysis of results. This high cost is common to almost all experiments, and leads to choosing a minimal (and as possible orthogonal) set of samples of the input set, leading to DOE. This DOE, more economical than the Monte Carlo trials, was chosen for the present work.

2.3. Conclusions of the Literature Review

In our literature survey, we found that the geometry of lattice structures implies the use of small FEA elements which produce intractable FEA meshes. Consequently, the numerical analysis of large lattice structures is a complex (sometimes unfeasible) process, limited by its elevated computational cost.

To alleviate the computational burden of the simulation of lattice structures, material homogenization is applied to produce regular domains that mimic the lattice domain. Following this approach, one can obtain fast and accurate approximations of the displacements field of the lattice domain. However, the stress–strain response cannot be directly obtained due to the geometric dissimilarities between the lattice and the homogeneous domains.

Our goal with this paper is to contribute to the problem of the estimation of the stress–strain response in large lattice domains. For this purpose, we propose a methodology that integrates material homogenization and DOE. We use the DOE-based methodology in [5] to devise simple mathematical expressions (meta-models) to characterize the stress–strain of Schwarz primitive lattice domains. The inputs of the produced meta-models are displacement-based features that can be efficiently calculated using material homogenization instead of full FEA simulations. The meta-models developed in this article are not intended to be suitable in high precision contexts, but to produce rough and efficient estimations of the von Mises stress that allow fast pre-evaluation of designs.

Particularly, we apply our methodology to estimate the von Mises stress under compressive loads for large (more than 100 cells) Schwarz primitive lattice structures. The meta-models use the strains of the boundary of the lattice cell to relate the displacement field of the homogeneous domain with the von Mises stress of the lattice domain.

3. Methodology

3.1. Schwarz Primitive Lattice Structures

Schwarz primitive lattice structures are obtained by calculating isosurfaces of the real-valued function $F : \mathbb{R}^3 \rightarrow \mathbb{R}$ in Equation (1):

$$F(x,y,z) = cos\left(\frac{2\pi}{L}x\right) + cos\left(\frac{2\pi}{L}y\right) + cos\left(\frac{2\pi}{L}z\right), \quad (1)$$

where L is the desired length of the cell [25].

Schwarz primitive lattice structures are employed in topology optimization for AM. The result of some common methods in topology optimization is a density map that is impossible to manufacture. The problem of converting that density map into a manufacturable domain does not have an exact solution. The mathematical structure of Schwarz primitive lattice allows for finding approximate solutions to that problem, providing manufacturable designs with smooth transitions in the connections of multiple cells, preventing stress concentration [7]. Moreover, Schwarz primitive lattice structures are stiffer than other lattice structures (such as the gyroid) [26]. These properties make Schwarz primitive structures attractive for engineering and biomedical applications [7,8,26].

In order to show the geometry of the Schwarz primitive cell, we obtained the isosurfaces for the isovalues $t = -0.87, 0.0, 0.87$; that is, we found the surfaces that solved the equation $F = t$. The corresponding relative densities (ρ; i.e., the ratio of the volume of the cell and L^3) of the cells were $\rho = 0.25, 0.5, 0.75$, respectively. Figure 1 displays the cells along with their corresponding isovalues and relative densities.

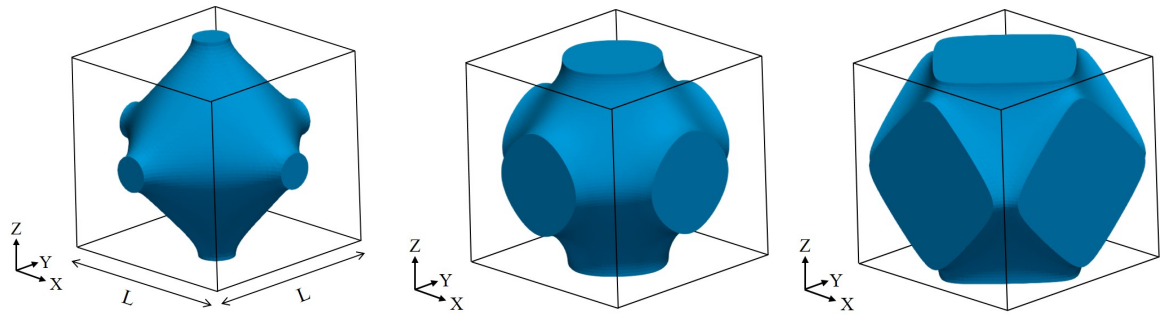

(**a**) (**b**) (**c**)

Figure 1. Geometry of Schwarz primitive cells. (**a**) Isovalue $t = -0.87$ and relative density $\rho = 0.25$; (**b**) isovalue $t = 0$ and relative density $\rho = 0.50$; and (**c**) isovalue $t = 0.87$ and relative density $\rho = 0.75$.

3.2. Methodology to Estimate the Stress–Strain Response of Lattice Structures

In this paper, we propose a methodology for the efficient estimation of the stress–strain response of large lattice structures. The proposed algorithm relies on two main concepts: material homogenization and DOE. The algorithm is divided into four stages: (1) material homogenization of the lattice structure, (2) numerical simulation of the load case using the homogeneous domain, (3) extraction of displacement-based features and (4) the application of meta-models to estimate the response variable based on the features extracted in (3). Below, we describe every step of our algorithm. Figure 2 presents a graphical summary of the proposed methodology, with the inputs and outputs of each phase of the process.

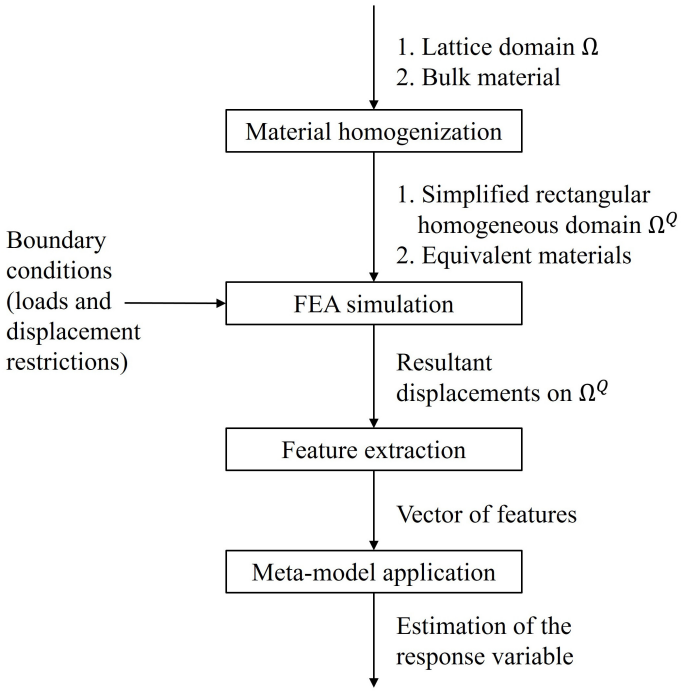

Figure 2. Work-flow for the estimation of the mechanical response of lattice domains using material homogenization and design of experiments (DOE).

3.2.1. Material Homogenization

This process seeks to obtain a simplified regular (homogeneous) domain Ω^Q that approximates the heterogeneous lattice structure Ω. The goal is to find an equivalent material $\left(E^Q, \nu^Q\right)$ so that the regular domain equipped with the equivalent material $\left(E^Q, \nu^Q\right)$ resembles the displacement field of the original lattice domain. We implemented the numerical homogenization method presented in [27], which has been applied in the context of lattice structures in [6,12]. In Section 3.3, the reader can find more details on the foundations of material homogenization.

3.2.2. FEA Simulation of the Homogeneous Domain

At this stage, the load case is simulated on the homogeneous domain Ω^Q using analogous boundary conditions. The result of this stage is the displacement field on Ω^Q, which is an approximation of the displacement field on the lattice domain Ω.

3.2.3. Feature Extraction

Characteristic features of every cell of the lattice domain Ω are extracted using the displacement field over the homogeneous domain Ω^Q obtained in the previous step. These displacement-based features extracted at this stage are used as inputs of the meta-models to estimate the stress–strain response of each cell. The definition of these features is central to obtaining reliable meta-models and is highly dependent on the expertise of the modeler.

The extracted features condense (or characterize) the deformation of the cell and must provide information about the variable of interest. In this work, we use as features the average normal strain at the flat faces of the boundary of the Schwarz primitive cells, which can be obtained directly from the displacements on the homogeneous domain Ω^Q. A discussion on how to generate the meta-models using DOE is presented in Section 3.4.

3.2.4. Meta-Model Execution

A meta-model is a simple mathematical expression (i.e., function) that relates the features extracted in the previous stage and the response variable. In other words, the features extracted in the previous stage (denoted by $\boldsymbol{X} = [x_1, \ldots, x_n]^T$) are used to feed a function $f : \mathbb{R}^n \to \mathbb{R}$ that gives an estimation of the response variable for every cell of the lattice domain. In this article, the meta-models are developed using DOE techniques (see Section 3.4).

3.3. Material Homogenization

Material homogenization seeks to represent a heterogeneous material with a simple *homogeneous* material. In the case of lattice structures, a lattice unit cell can be treated as a composite material formed by solid (with bulk properties E and ν) and void (with properties E_0 and ν_0) zones [6,12]. Material homogenization aims to find the material properties (E^Q and ν^Q) that make a filled cube behave like the unit lattice cell (see Figure 3).

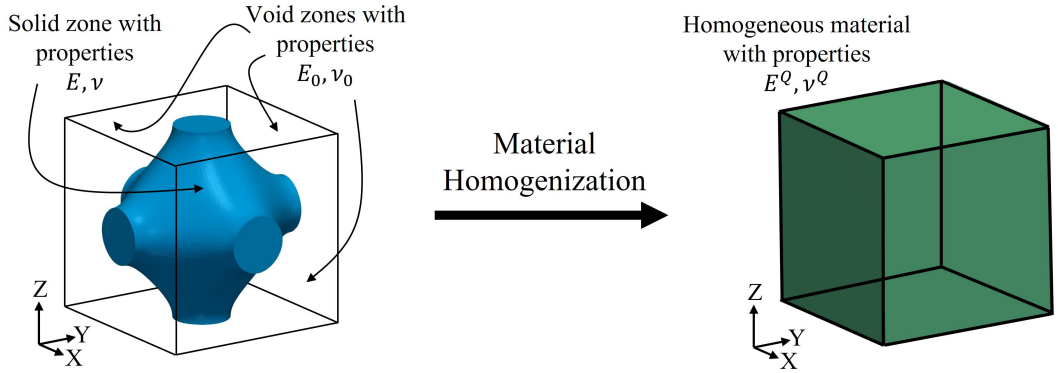

Figure 3. Graphical representation of material homogenization.

We implemented the numerical homogenization method proposed in [27]. This method finds the elasticity matrix $\boldsymbol{C}^Q$:

$$\boldsymbol{C}^Q = \begin{bmatrix} c_1 & c_2 & c_2 & 0 & 0 & 0 \\ c_2 & c_1 & c_2 & 0 & 0 & 0 \\ c_2 & c_2 & c_1 & 0 & 0 & 0 \\ 0 & 0 & 0 & c_3 & 0 & 0 \\ 0 & 0 & 0 & 0 & c_3 & 0 \\ 0 & 0 & 0 & 0 & 0 & c_3 \end{bmatrix}, \tag{2}$$

that relates stresses and strains in the homogeneous material as $\boldsymbol{\sigma} = \boldsymbol{C}^Q \boldsymbol{\varepsilon}$. The corresponding Young E^Q and Poisson ν^Q moduli are provided by the following equations:

$$E^Q = \frac{c_1^2 + c_1 c_2 - 2c_2^2}{c_1 + c_2}, \tag{3}$$

$$\nu^Q = \frac{c_2}{c_1 + c_2}. \tag{4}$$

In this work, we selected the titanium alloy *Ti-6Al-4V* as the bulk material with properties: Young's modulus $E = 114$ GPa and Poisson's ratio $\nu = 0.33$. We applied the homogenization procedure to obtain the diluted properties of Schwarz primitive cells for the relative densities $\rho \in \{0.25, 0.3, 0.4, 0.5, 0.6, 0.7, 0.8, 0.9\}$. Table 1 displays the results obtained. Table 1 also includes the case in which the density is $\rho = 1.0$. Notice that the properties of the homogeneous domain

coincide with the bulk properties (as expected). When needed, the properties of intermediate densities were obtained via linear interpolation.

Table 1. Results of numerical homogenization of Schwarz primitive cells: Young's modulus and Poisson's ratio.

Relative Density (ρ)	Equivalent Young's Modulus (E^Q)	Equivalent Poisson's Ratio (ν^Q)
0.25	7.5 GPa	0.05
0.3	14.0 GPa	0.09
0.4	24.0 GPa	0.13
0.5	35.0 GPa	0.17
0.6	48.0 GPa	0.21
0.7	61.0 GPa	0.23
0.8	81.0 GPa	0.27
0.9	97.0 GPa	0.29
1.0	114 GPa	0.33

3.4. Generation of Meta-Models Using DOE

DOE is a traditional and effective methodology based on statistical techniques that supports the analysis of complex processes and systems. DOE allows one to establish in a systematic way how changes in the parameters of a system or function affect their outcome, minimizing the uncertainty and the number of required experiments to complete such characterization. DOE covers the whole spectrum, from the planing of the experiments to the statistical analysis of the results [28,29]. We used DOE techniques to develop meta-models to estimate the von Mises stress in Schwarz primitive lattice structures.

The von Mises stress σ_{VM} is a material failure criterion used in the design and analysis of lattice structures in various works (e.g., [30–32]). The von Mises stress is defined per Equation (5):

$$\sigma_{VM} = \sqrt{\sigma_1^2 + \sigma_2^2 + \sigma_3^2 - (\sigma_1\sigma_2 + \sigma_1\sigma_3 + \sigma_2\sigma_3)}, \tag{5}$$

where $\sigma_1, \sigma_2, \sigma_3$ are the principal stresses. The criterion states that, for preventing failure, the von Mises stress must be below the tensile strength of the material. However, failure in lattice materials is also governed by buckling instabilities that occur before material failure [13]. For the sake of demonstration of the methodology, this work is limited to the estimation of the von Mises stress, although a more complete failure criterion for lattice structures should consider buckling phenomena.

The procedure to devise meta-models using DOE is summarized in three phases: (1) identification of potential features (also called factors) that may affect the variable of interest, (2) selection of the most influential (main) factors and (3) development of simple mathematical expressions (meta-models) that relate the main factors and the response variable.

We applied DOE to develop meta-models for the von Mises stress in Schwarz primitive lattice structures of different relative densities. In an ideal case, we should have attained a meta-model for each relative density $\rho \in (0, 1)$. This computational demand makes this option unfeasible. Since we were only seeking approximations of the von Mises stress, we found meta-models for the relative densities $\rho = 0.25, 0.50, 0.75, 1.0$. To find the four meta-models, we used lattice domains formed by a single unit cell of the mentioned relative densities. Below, we describe in detail every stage of the procedure.

3.4.1. Factor Identification

The goal at this stage was to detect features (or factors) $F_V = \{f_1, f_2, \cdots, f_n\}$ that (1) were related to the von Mises stress and (2) could be controlled. Additionally, the features had to be based on the displacements over the lattice, so that they could be retrieved from the FEA simulation over the homogeneous domain Ω^Q.

Our set of factors initially contained the strains at the flat faces (extreme faces) of the boundary of each unit cell of the Schwarz primitive lattice domain. For convenience, the flat faces of the boundary were denoted as $\{X, -X, Y, -Y, Z, -Z\}$. $\{-X, -Y, -Z\}$ were the flat faces at $x = 0, y = 0, z = 0$. $\{X, Y, Z\}$ were the flat faces at $x = L, y = L, z = L$. We defined the strains at the flat faces as:

$$\begin{aligned} \varepsilon_{ij} &= \mathrm{sgn}(i) \cdot \frac{U_{ij} - U_{-jj}}{L}, \\ i &= \pm X, \pm Y, \pm Z, \quad j = x, y, z, \end{aligned} \tag{6}$$

where U_{ij} represented the average displacement in j direction of the face i. For instance, U_{-Xx} was the displacement in x direction of the flat face at $x = 0$. The normal strains at the flat faces corresponded to $\{\varepsilon_{-Xx}, \varepsilon_{Xx}, \varepsilon_{-Yy}, \varepsilon_{Yy}, \varepsilon_{-Zz}, \varepsilon_{Zz}\}$. However, from Equation (6), $\varepsilon_{-Xx} = \varepsilon_{-Yy} = \varepsilon_{-Zz} = 0$, which prevented the introduction of false strains due to pure translation of the Schwarz primitive cell.

In Equation (5) we can see that the von Mises stress depends on the shear stress, and therefore, it is influenced by the shear strain. We conducted preliminary tests considering shear strains at the flat faces of the cell but our results overestimated the von Mises stress by a large factor. We found that the shear strain interaction is not fully understood at the level of DOE. Consequently, our set of factors was reduced to the normal strains at the flat faces of the cell $\{\varepsilon_{Xx}, \varepsilon_{Yy}, \varepsilon_{Zz}\}$.

3.4.2. Factor Selection

In the context of DOE, the goal at this stage is to reduce the number of considered factors, selecting those factors that affect the most the response variable. Mature techniques do exist for this task, such as full or fractional factorial or Plackett–Burman designs [28,29]. However, we considered only three factors, so we decided to develop the meta-models using all of them.

3.4.3. Meta-Model Development

The goal at this stage was to develop efficient and simple mathematical expressions that expressed the von Mises stress in Schwarz primitive lattice domains in terms of $\{\varepsilon_{Xx}, \varepsilon_{Yy}, \varepsilon_{Zz}\}$.

We used response surface methodologies, specifically central composite face-centered design (CCF), to efficiently devise the meta-models. The shape of the devised meta-models for Schwarz primitive cells of relative densities $\rho \in \{0.25, 0.5, 0.75\}$ was

$$\hat{y} = \left(\beta_0 + \sum_{i \leq j} \beta_{ij} \varepsilon_{ii} \varepsilon_{jj}\right)^2, \tag{7}$$

and the shape of the meta-model for $\rho = 1.0$ was

$$\hat{y} = \sqrt{\beta_0 \left(\sum_i \varepsilon_{ii}^2 - \sum_{i<j} \varepsilon_{ii} \varepsilon_{jj}\right)}. \tag{8}$$

We used `R` [33] to perform the regression analysis to estimate the coefficients (β_i, β_{ij}) of the meta-models (see Table 2).

To evaluate the meta-models, we ran 100 random simulations for each of the four domains and compared the experimental (result of FEA) and predicted (result of the meta-model) von Mises stress. The values of the Young's modulus and Poisson's ratio used for the simulations with the homogeneous domains were the ones reported in Table 1. For the cell of density $\rho = 0.75$, we used $E^Q = 71.0$ GPa and $\nu^Q = 0.25$, which resulted by interpolating the corresponding moduli of the cells of densities $\rho = 0.7$ and $\rho = 0.8$. We used the displacements on the homogeneous domains to calculate the normal strains at the flat faces ε_{ij} and used them as inputs for the meta-models in Equations (7) and (8).

The boundary conditions imposed on the four domains were prescribed displacements in the normal direction of the flat faces of the domains. The size of the cell used was $L = 1.0$ cm, so that the imposed displacements were equivalent to normal strains at the flat faces (ε_{ij}).

Our analysis was limited to the elastic zone of the material. The range of the variables was $\varepsilon_{ij} \in 10^{-5} \times [-1.0, 1.0]$. The values of the variables were coded in the range $[-1, 1]$ to be in concordance with the procedures found in the literature [29]. To ensure that the strains in the flat faces were in the working range $(\varepsilon_{ij} \in 10^{-5} \times [-1.0, 1.0])$ and to explore it evenly, the values of the imposed normal strains at the flat faces were generated from a uniform distribution in the interval $(-1.0 \times 10^{-5}, 1.0 \times 10^{-5})$.

Figure 4 displays the aforementioned comparison for each cell. We can see that the meta-models for the densities $\rho \in \{0.25, 0.50, 0.75\}$ tend to overestimate the von Mises stress at low stress conditions. This is due to the term β_0 in Equation (7), which impedes the meta-model to predict small values of von Mises stress. Table 2 gives the average and maximum relative error of the predicted vs. the experimental von Mises stress. The maximum relative errors are associated to low stress conditions, mainly influenced by the value of β_0 in Equation (7) (as previously discussed). It is clear that the meta-models are not well-suited for low stress conditions. The average and maximum relative errors in the estimations show that this methodology is not applicable in very sensitive processes where high accuracy is required.

Table 2. Values of the coefficients β in the fitted meta-models. Average and maximum relative errors between FEA and our approach for 100 random simulations.

Relative Density	β_0	β_{12}	β_{13}	β_{23}	β_{11}	β_{22}	β_{33}	Average Relative Error	Max. Relative Error
0.25	0.0438	0.0010	0.0013	0.0005	0.0089	0.0075	0.0067	19%	370%
0.50	0.0369	0.0019	0.0021	0.0019	0.0076	0.0073	0.0074	20%	298%
0.75	0.0419	0.0041	0.0039	0.0036	0.0089	0.0098	0.0091	21%	255%
1.0	0.4036	N/A	N/A	N/A	N/A	N/A	N/A	0%	0%

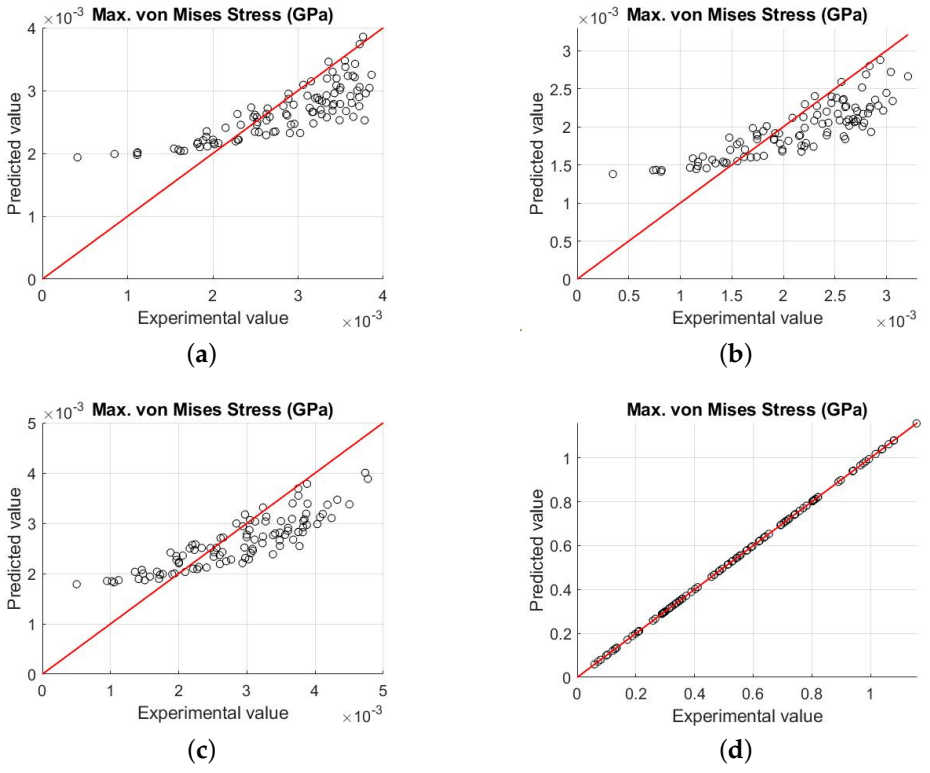

Figure 4. Experimental (result of lattice FEA) vs. predicted (result of the meta-model) von Mises stress in Schwarz primitive lattices of relative density (**a**) $\rho = 0.25$; (**b**) $\rho = 0.50$; (**c**) $\rho = 0.75$; and (**d**) $\rho = 1.0$.

4. Results

4.1. Validation of the Proposed Methodology

To evaluate our methodology, we compared the results of the FEA simulation and our methodology for six Schwarz primitive lattice domains. Three of the six domains (Figure 5a–c) were formed by eight unit cells of uniform density $\rho = 0.25, 0.50, 0.75$, respectively. The other three domains were formed by unit cells of graded density; that is, the isovalue t was not a constant but a function $t : \mathbb{R}^3 \rightarrow \mathbb{R}$. The resultant surfaces are the solutions to Equation $F(x,y,z) = t(x,y,z)$ (see Equation (1)). The domain of 24 unit cells in Figure 5f was taken from [7] and corresponded to the result of mapping the results of topology onto Schwarz primitive cells [7]. The domains of eight cells displayed in Figure 5d,e were also taken from [7]. The isovalue functions associated with these two domains are:

$$t(x,y,z) = \begin{cases} -\frac{5}{2}\left(\frac{3x}{2L}\right)^2 + 2 & , 0 \leq x \leq \frac{2L}{3}, y, z \in \mathbb{R} \\ -\frac{1}{2} & , \frac{2L}{3} < x \leq \frac{4L}{3}, y, z \in \mathbb{R} \\ \frac{3}{2L}x - \frac{5}{2} & , \frac{4L}{3} < x \leq 2L, y, z \in \mathbb{R} \end{cases} \quad (9)$$

$$t(x,y,z) = 3\left(\frac{x}{L} - 1\right)^2 - \frac{1}{2}, \quad 0 \leq x \leq 2L, y, z \in \mathbb{R} \quad (10)$$

The six domains were subjected to uniaxial compression (see Figure 5). The magnitude of the load was such that the resultant strains in the flat faces of the boundary of the cells lay in the range of analysis $\varepsilon_{ij} \in 10^{-5} \times [-1.0, 1.0]$. First, we compared the displacements field of the lattice and homogeneous domain (Section 4.1.1). Secondly, we applied our DOE-based methodology using the displacement results from the homogeneous domain to get the maximum von Mises stress in every cell. Finally, we compared the maximum von Mises stress obtained via (1) direct FEA of the lattice domain and (2) our proposed methodology (Section 4.1.2).

4.1.1. Material Homogenization in Schwarz Primitive Lattice Structures

The FEA simulations of the lattice and homogeneous domains were executed in ANSYS. The lattice models were meshed in ANSYS using tetrahedral elements (`SOLID285`). The material properties of the lattice models correspond to the bulk material properties ($\rho = 1.0$ in Table 1). On the other hand, given the regular shape of the homogeneous domains, we used cubic elements (`SOLID185`) for the respective meshes. Each cubic sub-domain was isotropic and its material properties were assigned according to its relative density and the properties reported in Table 1. The homogeneous domain was then a regular 3D array of isotropic cubic sub-domains. Since the properties of each sub-domain could be different, the homogeneous domain resulted to be anisotropic.

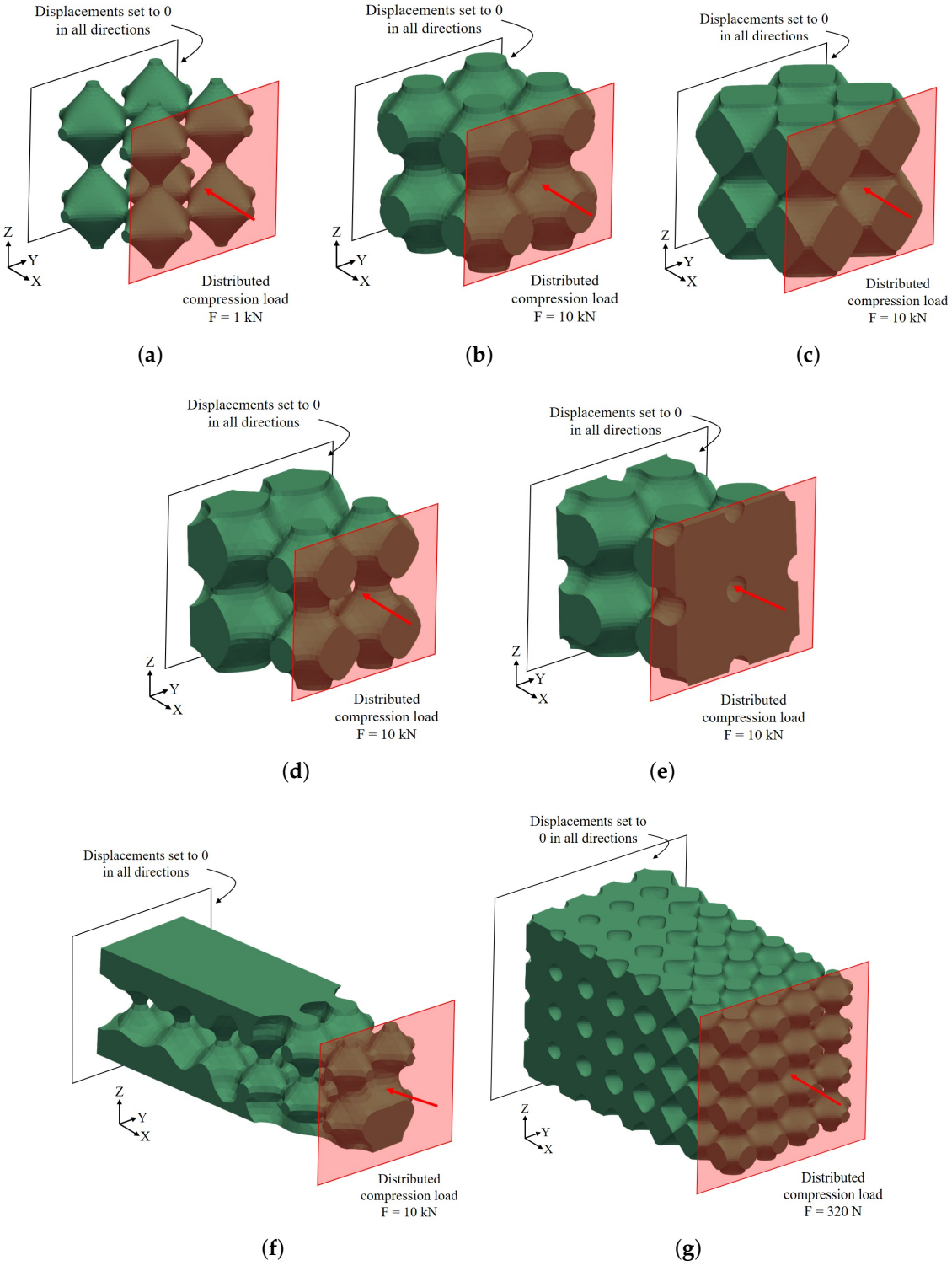

Figure 5. Studied domains and boundary conditions for the FEA simulations. Domains of eight cells of uniform density (**a**) $\rho = 0.25$; (**b**) $\rho = 0.50$; and (**c**) $\rho = 0.75$. Domains of eight cells of density (**d**) per Equation (9); and (**e**) per Equation (10). (**f**) Domain of 24 cells with density per [7]. (**g**) Domain of 112 cells with density per Equation (12).

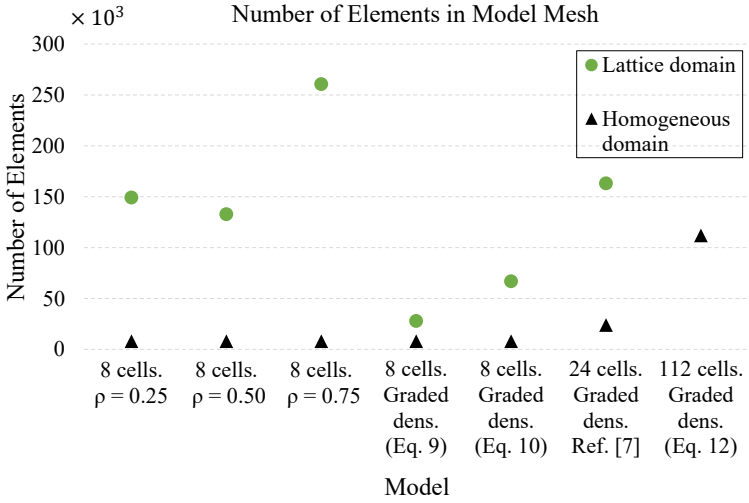

Figure 6. Number of elements in the FE meshes of lattice and simplified homogeneous domains.

FEA simulations were executed using different hardware settings and different operative systems; therefore, it was not possible to compare execution times between different simulations in equal conditions. To overcome this difficulty, we used the number of elements in the mesh as a measurement of computational expense in each domain. The numbers of elements required for each lattice and each homogeneous domain are reported in Figure 6 and Table 3. It is noticeable that the FEA meshes of lattice domains required more elements than the homogeneous domains. Another important aspect to highlight is that the number of elements of the homogeneous domain only depend on the number of cells (particularly, we chose a mesh of $10 \times 10 \times 10$ elements per unit cell). On the other hand, the number of elements for the lattice domains does not completely depend on the number of cells. Notice that five out of the six domains are conformed by eight unit cells. However, the number of elements (Figure 6 and Table 3) is different for each domain. These variations are mainly influenced by the shape of the domain, which affects the corresponding meshing algorithms of the FEA software (ANSYS).

Table 3. Number of elements in FE meshes of lattice and simplified homogeneous domains.

Domain	Figure Number	No. of Elements in Lattice Domain	No. of Elements in Homogeneous Domain
8 cells. Uniform density with $\rho = 0.25$	Figure 5a	149,090	8000
8 cells. Uniform density with $\rho = 0.50$	Figure 5b	132,710	8000
8 cells. Uniform density with $\rho = 0.75$	Figure 5c	260,610	8000
8 cells. Graded density per Equation (9)	Figure 5d	27,863	8000
8 cells. Graded density per Equation (10)	Figure 5e	66,890	8000
24 cells. Graded density per [7]	Figure 5f	163,080	24,000
112 cells. Graded density per Equation (12)	Figure 5g	N/A	112,000

After conducting the FEA simulations, we proceeded to compare the resultant displacements of the lattice and homogeneous domains. Figures 7 and 8 (1) contrast the nodal displacement in the load direction X for the six load cases and (2) show the absolute difference between the X displacement predicted by the lattice and homogeneous approaches. The reader may observe the similarity in both the distribution and magnitude of the displacements field of the lattice and homogeneous domains. Figures 7 and 8 also show that the maximum value of the absolute error is in all cases approximately 10 times smaller than the maximum displacement. From these results we conclude that material homogenization is an accurate tool to estimate the displacements in lattice structures and its efficiency allows its application in large lattice domains.

4.1.2. Comparison between FEA and Our Methodology

We used the displacements on the homogeneous domains obtained in the previous stage to extract the inputs of our meta-models: the normal strains on the boundary of each cell. Then,

we used the meta-models presented in Section 3.4 to estimate the maximum von Mises stress in each cell. To apply the meta-models, we calculated the average relative density of each cell of the non-uniform (graded) density domains. Since we had only meta-models for the relative densities $\rho \in \{0.25, 0.50, 0.75, 1.0\}$, we used linear interpolation to do the approximations for the intermediate values of density ρ. For instance, $\left(\sigma_{VM}^{(0.4)}\right)$, the von Mises stress for a relative density $\rho = 0.4$ is approximated as

$$\sigma_{VM}^{(0.4)} = \frac{2}{5}\sigma_{VM}^{(0.25)} + \frac{3}{5}\sigma_{VM}^{(0.5)}, \tag{11}$$

where $\sigma_{VM}^{(0.25)}$ and $\sigma_{VM}^{(0.50)}$ denote the von Mises stresses for the cells of densities $\rho = 0.25$ and $\rho = 0.50$. $\sigma_{VM}^{(0.25)}$ and $\sigma_{VM}^{(0.50)}$ are retrieved using Equation (7) with the corresponding coefficients of Table 2.

Figures 9 and 10 show (i) the von Mises stress of the FEA simulation, (ii) the maximum von Mises stress of every cell retrieved from the FEA simulation of the lattice domain and (iii) the maximum von Mises stress of every cell calculated with our methodology. In addition, Table 4 lists, for each domain, the global maximum von Mises stress using (a) FEA simulation of the lattice domain and (b) our methodology. We measured the relative error of our methodology with respect to the FEA simulation of the lattice domain. These results are reported also in Table 4.

In Figures 9 and 10, we can see that the maximum von Mises stress given by our methodology (third column of the figures) is very uniform along all the cells. When compared with the maximum von Mises stress of the FEA methodology (second column of the figures), it is clear that our methodology is not able to capture all the variations of the maximum von Mises stress per cell (see Figure 10h,i). However, we can see the correspondence between the most stressed zones using FEA simulation and our methodology. Note that our implementation often predicts the most stressed cell.

Table 4. Maximum von Mises stress values of direct FEA of the lattice domain vs. our methodology.

Domain	Figure Number	Max. σ_{VM}: FEA (MPa)	Max. σ_{VM}: Our Method (MPa)	Rel. Error
Eight cells. Uniform density with $\rho = 0.25$	Figure 5a	3.6	2.4	33%
Eight cells. Uniform density with $\rho = 0.50$	Figure 5b	4.5	3.6	20%
Eight cells. Uniform density with $\rho = 0.75$	Figure 5c	3.4	2.4	29%
Eight cells. Graded density per Equation (9)	Figure 5d	3.1	3.6	16%
Eight cells. Graded density per Equation (10)	Figure 5e	3.4	2.8	17%
24 cells. Graded density per [7]	Figure 5f	3.1	1.8	42%

In terms of the accuracy of our methodology, we can see in Table 4 that (1) the error in the estimations with our methodology is between 16% and 42% and (2) our methodology tends to underestimate the maximum von Mises stress. These results show that our methodology can only do rough estimations (with errors above 20%) of the maximum von Mises stress in Schwarz lattice structures.

We have identified three critical aspects that can improve the accuracy of our methodology:

1. To consider more displacement-based features located inside the cell, not only on the boundary of the cell.
2. To develop meta-models for more relative densities. Currently, it is limited to meta-models of density $\rho \in \{0.25, 0.50, 0.75, 1.0\}$.
3. To enlarge the range of analysis of the displacement-based features, since in a single load case, the magnitude of the deformation of the lattice domain varies in every zone. Currently, the allowed normal strains are limited to the interval $10^{-5} \times [-1.0, 1.0]$.

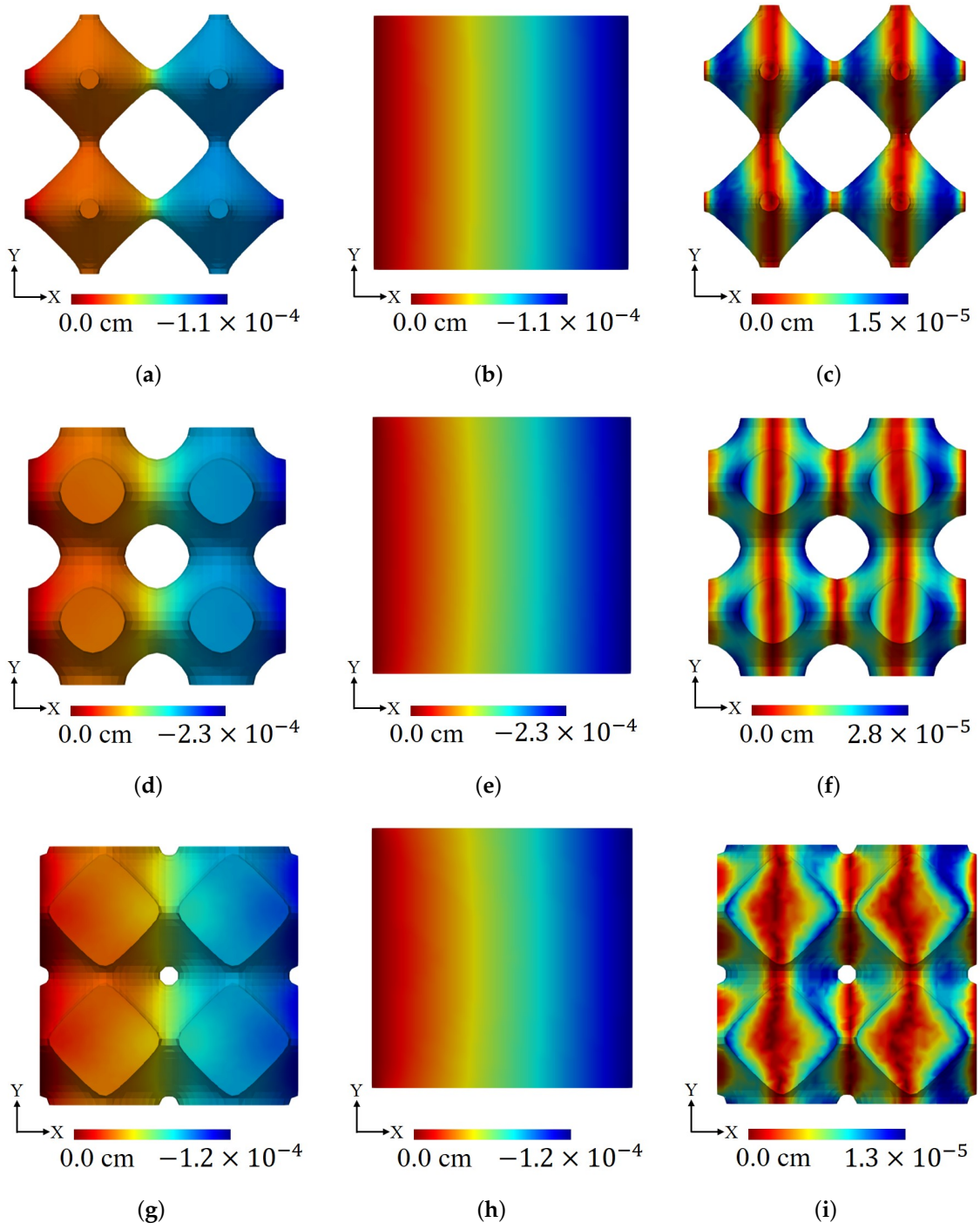

Figure 7. Results of X compression test. Domains of eight cells domains of uniform density. Domain of $\rho = 0.25$: (**a**) X displacement in lattice domain. Min. displacement: -1.1×10^{-4} cm; (**b**) X displacement in homogeneous domain. Min. displacement -1.1×10^{-4} cm; and (**c**) absolute error. Domain of $\rho = 0.50$: (**d**) X displacement in lattice domain. Min. displacement: -2.3×10^{-4} cm; (**e**) X displacement in homogeneous domain. Min. displacement -2.2×10^{-4} cm; and (**f**) absolute error. Domain of $\rho = 0.75$: (**g**) X displacement in lattice domain. Min. displacement: -1.2×10^{-4} cm; (**h**) X displacement in homogeneous domain. Min. displacement -1.1×10^{-4} cm; and (**i**) absolute error.

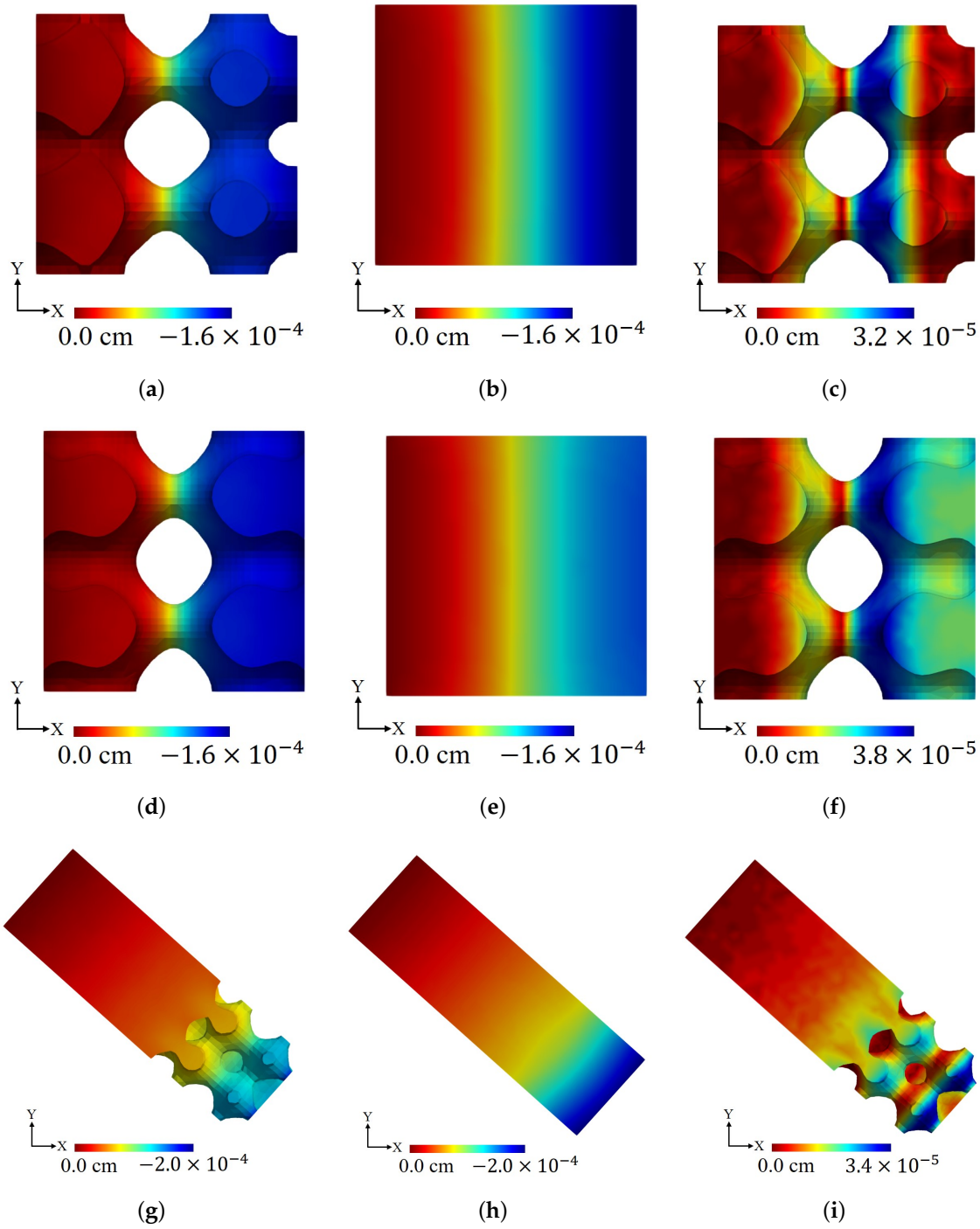

Figure 8. Results of X compression test. Domains of graded density of 8 and 24 cells. Domain of density per Equation (9): (**a**) X displacement in lattice domain. Min. displacement: -1.6×10^{-4} cm; (**b**) X displacement in homogeneous domain. Min. displacement -1.6×10^{-4} cm; and (**c**) absolute error. Domain of density per Equation (10): (**d**) X displacement in lattice domain. Min. displacement: -1.6×10^{-4} cm; (**e**) X displacement in homogeneous domain. Min. displacement -1.3×10^{-4} cm; and (**f**) absolute error. Domain of density as in [7]: (**g**) X displacement in lattice domain. Min. displacement: -1.8×10^{-4} cm; (**h**) X displacement in homogeneous domain. Min. displacement -2.0×10^{-4} cm; and (**i**) absolute error.

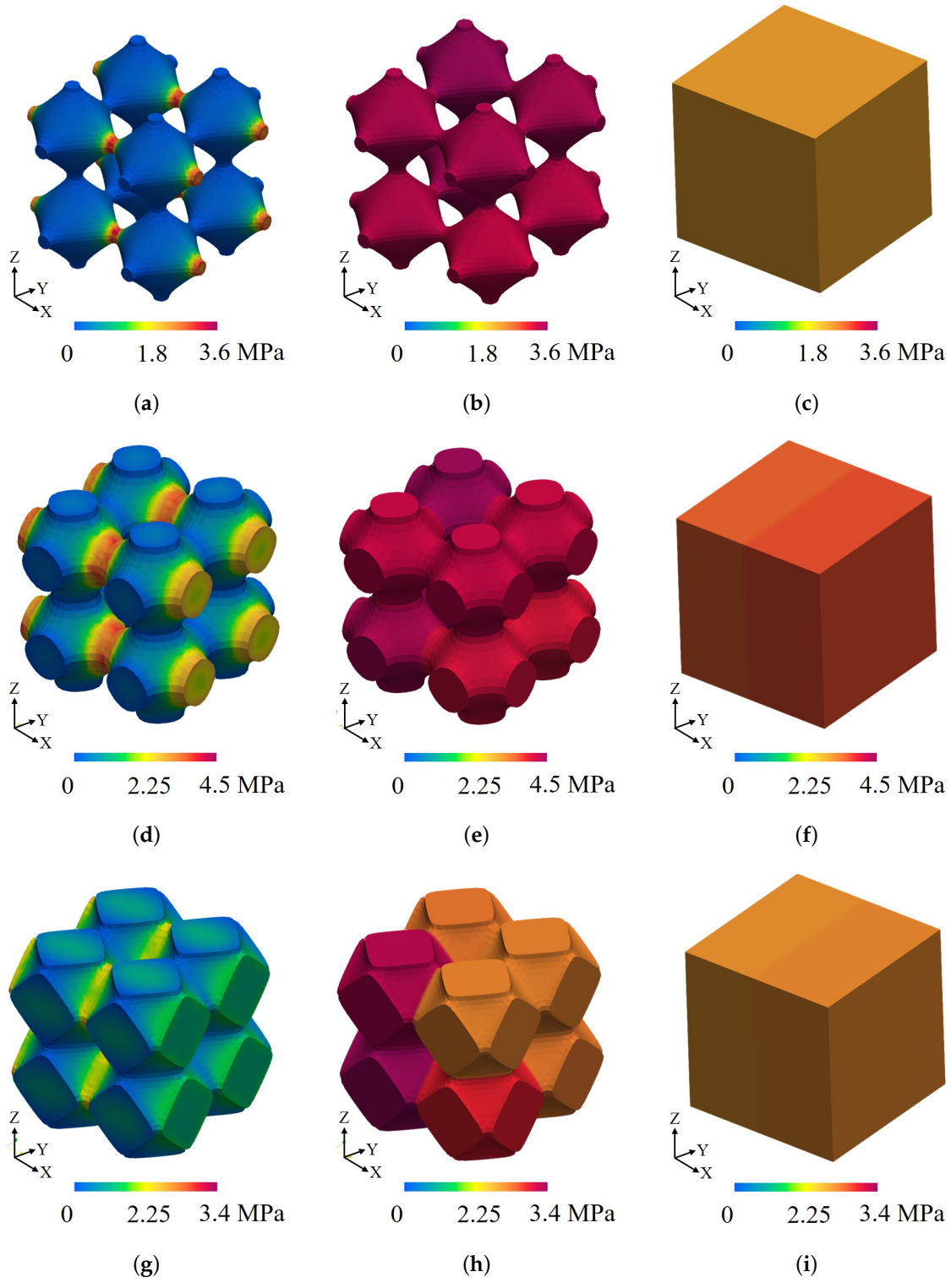

Figure 9. Comparison of the maximum von Mises stress in direct FEA (lattice) and our methodology in Schwarz primitive structures. Domains of eight cells of uniform density. Distribution of von Mises stress in lattice domain with (**a**) $\rho = 0.25$; (**d**) $\rho = 0.50$; and (**g**) $\rho = 0.75$. Maximum von Mises stress per cell in lattice domain with (**b**) $\rho = 0.25$; (**e**) $\rho = 0.50$; and (**h**) $\rho = 0.75$. Maximum von Mises stress per cell in homogeneous domain with (**c**) $\rho = 0.25$; (**f**) $\rho = 0.50$; and (**i**) $\rho = 0.75$. Detailed results in Table 4.

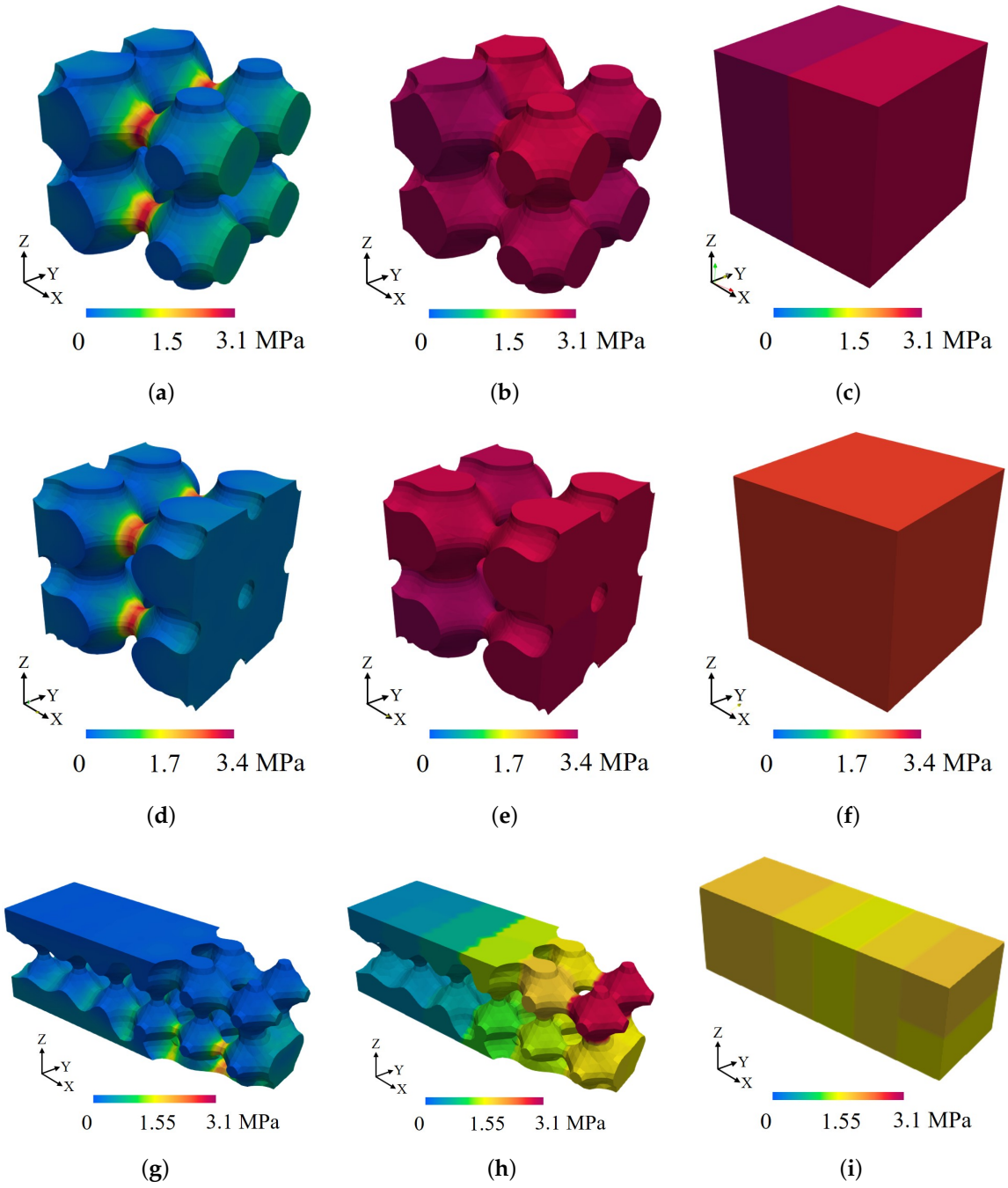

Figure 10. Comparison of the maximum von Mises stress in direct FEA (lattice) and our methodology in Schwarz primitive structures of graded density. Domains of 8 and 24 cells. Distribution of von Mises stress in lattice domain with (**a**) density per Equation (9); (**d**) density per Equation (10); and (**g**) density as in [7]. Maximum von Mises stress per cell in lattice domain with (**b**) density per Equation (9); (**e**) density per Equation (10); and (**h**) density as in [7]. Maximum von Mises stress per cell in homogeneous domain with (**c**) density per Equation (9); (**f**) density per Equation (10); and (**i**) density as in [7]. Detailed results in Table 4.

4.2. Application of Our Methodology to Large Lattice Domains

To demonstrate the potential of our methodology to be applied in the roughly estimation of the von Mises stress in larger lattice structures, we generated a domain of 112 ($7 \times 4 \times 4$) cells of graded

density. We tested it under uniaxial compression in X direction (Figure 11a). The isovalue function associated to this domain is:

$$t(x, y, z) = 2.5 - \frac{0.3}{L}(x + y). \tag{12}$$

First, we produced the homogeneous domain and conducted the FEA simulation. The number of elements of the mesh was 112,000 ($10 \times 10 \times 10$ elements per cell). Secondly, using the displacements field (Figure 11b), we extracted the normal strains on the boundary of each of the 112 cells. Finally, we used the meta-models of Section 3.4 along with linear interpolation to estimate the maximum von Mises stress in each cell. The results of this estimation are shown in Figure 11c.

Due to the large number of cells (117), the FEA directly on the lattice domain was unfeasible. However, it is possible to show the computational efficiency of our approach: to mesh a lattice domain of 24 cells, 160 k elements were required (6.6 k elements per cell), while for the homogeneous domain of 112 cells, 112 k elements were used (1.0 k elements per cell). This example has shown the computational efficiency of our approach in comparison with direct FEA simulation. It shows that our approach has the potential to be employed in the estimation of the stress–strain response of large lattice domains.

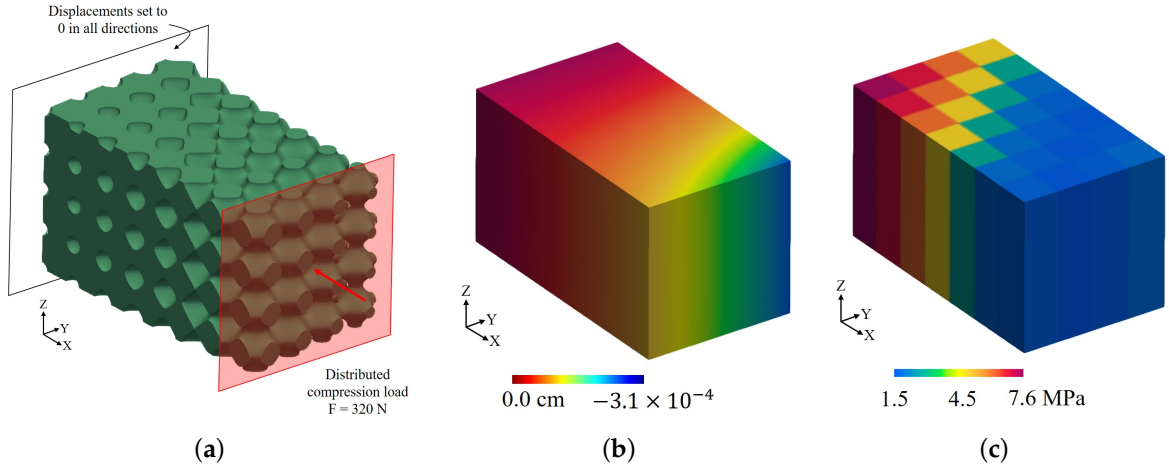

Figure 11. Application of our methodology to a large Schwarz primitive domain of 112 cells of density per Equation (12). (**a**) Domain and boundary conditions; (**b**) displacement in X direction in the homogeneous domain; and (**c**) maximum von Mises stress per cell in the homogeneous domain.

5. Conclusions

In this article we present a methodology that integrates material homogenization and design of experiments (DOE) to estimate the stress–strain responses in large lattice domains while reducing the computational cost with respect to direct FEA simulation. On the one hand, material homogenization is used to efficiently approximate the displacements on the lattice domains. On the other hand, DOE is applied to produce simple mathematical expressions to express the stresses in the lattice as functions of the displacements obtained through homogenization. In comparison with related approaches, this methodology is easy to implement, can be applied with different families of lattices (strut or surface based) and offers an efficient alternative to retrieve the stress–strain responses of complex lattice domains. However, it is less accurate and produces only rough estimations.

We implemented the proposed methodology to estimate the von Mises stress in Schwarz primitive lattice structures. Material homogenization proved its suitability for the approximation of the displacements in large lattice domains. Results have also shown that the proposed methodology is an efficient tool with potential applications in the *coarse* estimation of the von Mises stress in large lattice domains. The average errors in the estimations are between 20% and 40%, which *are not acceptable* in sensitive processes where high accuracy is required. However, these results are encouraging when

it is considered that we estimated meta-models for only four densities ($\rho \in \{0.25, 0.50, 0.75, 1.0\}$) for a narrow range of strains on the boundaries of the cells $10^{-5} \times [-1.0, 1.0]$. Our methodology has shown potential for the pre-evaluation of designs, where less precision is needed.

The methodology presented in this paper can be applied to other types of lattice structures (different to the Schwarz primitive). It will be necessary to develop meta-models for the lattice structures of interest, and consequently, to perform material homogenization to obtain the Young's and Poisson's moduli associated to the relative density.

Future Work

Future work is needed to improve the accuracy of the estimations of the von Mises stress. Efforts should be focused on the fitting of more robust meta-models that use more information from the displacements field obtained via material homogenization.

This paper considers the von Mises stress as a failure criterion for lattice domains. However, lattice structures at low densities experience buckling instabilities. This phenomenon should be considered to analyze failure in lattice structures.

Author Contributions: D.M.-Z., D.A.A. and O.R.-S. conceptualized and designed the algorithm. D.M.-Z. and J.P.-C. implemented the algorithm and executed the simulations. D.A.A. and A.M. supervised the design of experiments and statistical aspects of this research. C.C., J.P. and O.R.-S. supervised the computational geometry and computational mechanics aspects of this research. All the authors contributed to the writing of the article. All authors have read and agreed to the published version of the manuscript.

Funding: This research received no external funding.

Conflicts of Interest: The authors declare no conflict of interest.

Abbreviations

The following abbreviations are used in this manuscript:

AM	Additive manufacturing.
CCF	Central composite face-centered design.
DOE	Design of experiments.
FEA	Finite element analysis.
Ω, Ω^Q	Subsets of $\mathbb{R}^3$ that represents the lattice domain and the equivalent homogeneous domain, respectively $(\Omega, \Omega^Q \subset \mathbb{R}^3)$.
E, E^Q	Young's moduli of the bulk and equivalent material, respectively (Pa).
ν, ν^Q	Poisson's ratio of the bulk and equivalent material, respectively.
σ_{VM}	Von Mises stress (Pa).
L	Length of the Schwarz primitive cell $(L > 0)$.
ρ	Relative density or volume fraction of a Schwarz primitive cell $(0 \leq \rho \leq 1)$.
t	Iso-value used to generate the Schwarz primitive cell $(t \in [-3, 3])$.

References

1. Posada, J.; Toro, C.; Barandiaran, I.; Oyarzun, D.; Stricker, D.; de Amicis, R.; Pinto, E.B.; Eisert, P.; Döllner, J.; Vallarino, I. Visual Computing as a Key Enabling Technology for Industrie 4.0 and Industrial Internet. *IEEE Comput. Graph. Appl.* **2015**, *35*, 26–40. [CrossRef]
2. Helou, M.; Kara, S. Design, analysis and manufacturing of lattice structures: an overview. *Int. J. Comput. Integr. Manuf.* **2018**, *31*, 243–261. [CrossRef]
3. Cortés, C.; Osorno, M.; Uribe, D.; Steeb, H.; Ruiz-Salguero, O.; Barandiaran, I.; Flórez, J. Geometry simplification of open-cell porous materials for elastic deformation FEA. *Eng. Comput.* **2019**, *35*, 257–276. [CrossRef]
4. Terriault, P.; Brailovski, V. Modeling and simulation of large, conformal, porosity-graded and lightweight lattice structures made by additive manufacturing. *Finite Elem. Anal. Des.* **2018**, *138*, 1–11. [CrossRef]

5. Montoya-Zapata, D.; Acosta, D.A.; Cortés, C.; Pareja-Corcho, J.; Moreno, A.; Posada, J.; Ruiz-Salguero, O. Meta-modeling of Lattice Mechanical Responses via Design of Experiments. In Proceedings of the 2nd International Conference on Mathematics and Computers in Science and Engineering (MACISE 2020), Madrid, Spain, 18–20 January 2020.
6. Li, D.; Liao, W.; Dai, N.; Dong, G.; Tang, Y.; Xie, Y.M. Optimal design and modeling of gyroid-based functionally graded cellular structures for additive manufacturing. *Comput. Aided Des.* **2018**, *104*, 87–99. [CrossRef]
7. Montoya-Zapata, D.; Moreno, A.; Pareja-Corcho, J.; Posada, J.; Ruiz-Salguero, O. Density-Sensitive Implicit Functions Using Sub-Voxel Sampling in Additive Manufacturing. *Metals* **2019**, *9*. [CrossRef]
8. Panesar, A.; Abdi, M.; Hickman, D.; Ashcroft, I. Strategies for functionally graded lattice structures derived using topology optimisation for Additive Manufacturing. *Addit. Manuf.* **2018**, *19*, 81–94. [CrossRef]
9. Wu, J.; Wang, W.; Gao, X. Design and Optimization of Conforming Lattice Structures. *IEEE Trans. Vis. Comput. Graph.* **2019**, 1. [CrossRef]
10. Ataee, A.; Li, Y.; Fraser, D.; Song, G.; Wen, C. Anisotropic Ti-6Al-4V gyroid scaffolds manufactured by electron beam melting (EBM) for bone implant applications. *Mater. Des.* **2018**, *137*, 345–354. [CrossRef]
11. Melchels, F.P.; Bertoldi, K.; Gabbrielli, R.; Velders, A.H.; Feijen, J.; Grijpma, D.W. Mathematically defined tissue engineering scaffold architectures prepared by stereolithography. *Biomaterials* **2010**, *31*, 6909–6916. [CrossRef]
12. Cheng, L.; Zhang, P.; Biyikli, E.; Bai, J.; Robbins, J.; To, A. Efficient design optimization of variable-density cellular structures for additive manufacturing: theory and experimental validation. *Rapid Prototyp. J.* **2017**, *23*, 660–677. [CrossRef]
13. Liu, L.; Kamm, P.; García-Moreno, F.; Banhart, J.; Pasini, D. Elastic and failure response of imperfect three-dimensional metallic lattices: the role of geometric defects induced by Selective Laser Melting. *J. Mech. Phys. Solids* **2017**, *107*, 160–184. [CrossRef]
14. Park, S.I.; Rosen, D.W. Homogenization of Mechanical Properties for Material Extrusion Periodic Lattice Structures Considering Joint Stiffening Effects. *J. Mech. Des.* **2018**, *140*, 111414. [CrossRef]
15. Bonatti, C.; Mohr, D. Mechanical performance of additively-manufactured anisotropic and isotropic smooth shell-lattice materials: Simulations & experiments. *J. Mech. Phys. Solids* **2019**, *122*, 1–26. [CrossRef]
16. Lei, H.; Li, C.; Meng, J.; Zhou, H.; Liu, Y.; Zhang, X.; Wang, P.; Fang, D. Evaluation of compressive properties of SLM-fabricated multi-layer lattice structures by experimental test and μ-CT-based finite element analysis. *Mater. Des.* **2019**, *169*, 107685. [CrossRef]
17. Montoya-Zapata, D.; Cortés, C.; Ruiz-Salguero, O. FE-simulations with a simplified model for open-cell porous materials: A Kelvin cell approach. *J. Comput. Methods Sci. Eng.* **2019**, *19*, 989–1000. [CrossRef]
18. Tryland, T.; Hopperstad, O.S.; Langseth, M. Design of experiments to identify material properties. *Mater. Des.* **2000**, *21*, 477–492. [CrossRef]
19. Kovalovs, A.; Chate, A.; Gaidukovs, S.; Medvids, A. Finite Element Simulation of Indentation Experiment on Branched Epoxy Novolac Resin. *IOP Conf. Ser. Mater. Sci. Eng.* **2019**, *500*, 012006. [CrossRef]
20. Oliveira, L.Á.; Santos, J.C.; Panzera, T.H.; Freire, R.T.; Vieira, L.M.; Scarpa, F. Evaluation of hybrid-short-coir-fibre-reinforced composites via full factorial design. *Compos. Struct.* **2018**, *202*, 313–323. [CrossRef]
21. Phanphet, S.; Dechjarern, S.; Jomjanyong, S. Above-knee prosthesis design based on fatigue life using finite element method and design of experiment. *Med. Eng. Phys.* **2017**, *43*, 86–91. [CrossRef]
22. Schäfer, C.; Finke, E. Shape optimisation by design of experiments and finite element methods—An application of steel wheels. *Struct. Multidiscip. Optim.* **2008**, *36*, 477–491. [CrossRef]
23. Lozanovski, B.; Downing, D.; Tran, P.; Shidid, D.; Qian, M.; Choong, P.; Brandt, M.; Leary, M. A Monte Carlo simulation-based approach to realistic modelling of additively manufactured lattice structures. *Addit. Manuf.* **2020**, *32*, 101092. [CrossRef]
24. Mendenhall, W.M.; Sincich, T.L. *Statistics for Engineering and the Sciences*, 6th ed.; CRC Press: Boca Raton, FL, USA, 2016.
25. Wohlgemuth, M.; Yufa, N.; Hoffman, J.; Thomas, E.L. Triply Periodic Bicontinuous Cubic Microdomain Morphologies by Symmetries. *Macromolecules* **2001**, *34*, 6083–6089. [CrossRef]

26. Maskery, I.; Sturm, L.; Aremu, A.; Panesar, A.; Williams, C.; Tuck, C.; Wildman, R.; Ashcroft, I.; Hague, R. Insights into the mechanical properties of several triply periodic minimal surface lattice structures made by polymer additive manufacturing. *Polymer* **2018**, *152*, 62. [CrossRef]
27. Steven, G.P. Homogenization of multicomponent composite orthotropic materials using FEA. *Commun. Numer. Methods Eng.* **1997**, *13*, 517–531. [CrossRef]
28. Box, G.E.P.; Hunter, J.S.; Hunter, W.G. *Statistics for Experimenters: Design, Discovery, and Innovation*, 2nd ed.; Wiley Series in Probability and Statistics; Wiley: Hoboken, NJ, USA, 2005.
29. NIST/SEMATECH. e-Handbook of Statistical Methods. Available online: http://www.itl.nist.gov/div898/handbook/ (accessed on 4 December 2019).
30. Rizzuto, J. Experimental investigation of reciprocally supported element (RSE) lattice honeycomb domes structural behaviour. *Eng. Struct.* **2018**, *166*, 496–510. [CrossRef]
31. Yu, H.; Huang, J.; Zou, B.; Shao, W.; Liu, J. Stress-constrained shell-lattice infill structural optimisation for additive manufacturing. *Virtual Phys. Prototyp.* **2020**, *15*, 35–48. [CrossRef]
32. Ren, X.; Xiao, L.; Hao, Z. Multi-property cellular material design approach based on the mechanical behaviour analysis of the reinforced lattice structure. *Mater. Des.* **2019**, *174*, 107785. [CrossRef]
33. R Core Team. *R: A Language and Environment for Statistical Computing*; R Foundation for Statistical Computing: Vienna, Austria, 2019.